eprints@whiterose.ac.uk
https://eprints.whiterose.ac.uk/

**Astronomy
&
Astrophysics**

Stability of an MHD shear flow with a piecewise linear velocity profile

M. S. Ruderman[1] and L. Brevdo[2]

[1] Department of Applied Mathematics, University of Sheffield, Hicks Building, Hounsfield Road, Sheffield S3 7RH, UK
  e-mail: M.S.Ruderman@sheffield.ac.uk
[2] Université de la Méditerranée, IMT–Technopôle de Château-Gombert, 38 rue Frédéric Joliot Curie, 13451 Marseille Cedex 20, France

ABSTRACT

In this paper we present the results of the stability analysis of a simple shear flow of an incompressible fluid with a piecewise linear velocity profile in the presence of a magnetic field. In the flow, a finite transitional magnetic-free layer with a linear velocity profile is sandwiched by two semi-infinite regions. One of these regions is magnetic-free and the flow velocity in the region is constant. The other region is magnetic and the fluid in it is quiescent. The magnetic field is constant and parallel to the flow in the transitional layer. The fluid density is constant both in the magnetic as well as the magnetic-free regions, while it has a jump-type discontinuity at the boundary between the transitional layer and the magnetic region. The effect of gravity is included in the model, and it is assumed that the lighter fluid is overlaying the heavier one, thus no Rayleigh-Taylor instability is present. The dispersion equation governing the normal-mode stability of the flow is derived and its properties are analysed. We study stability of two cases: (i) magnetic-free flow in the presence of gravity, and (ii) magnetic flow without gravity. In the first case, the flow stability is controlled by the Rayleigh number, R. In the second case, the control parameter is the inverse squared Alfvénic Mach number, H. Stability of a particular monochromatic perturbation also depends on its dimensionless wavenumber α. We combine the analytical and numerical approaches to obtain the neutral stability curves in the (α, R)-plane in the case of the magnetic-free flow, and in the (α, H)-plane in the case of the magnetic flow. The dependence of the instability increment on R in the first case, and on H in the second case is treated. We apply the results of the analysis to the stability of a strongly subsonic portion of the heliopause. Our main conclusion is as follows: The inclusion of a transitional layer near the heliopause into the model increases by an order of magnitude the strength of the interstellar magnetic field required to stabilize this portion of the heliopause in comparison with the corresponding stabilizing strength of the magnetic field required when modelling the heliopause as a tangential discontinuity.

Key words. magnetohydrodynamics (MHD) – solar wind – instabilities – ISM: general

1. Introduction

Magnetohydrodynamic (MHD) shear flows are common in space plasmas. Well-known examples of such flows are the flows near the magnetopauses of the Earth and other planets, the flows close to the heliopause and the flows at the boundaries of the fast and slow streams of the solar wind. Also some flows observed in the solar atmosphere can be treated as shear flows. Studying stability of MHD shear flows is of a considerable importance for the understanding of the physical processes in space plasmas and for a correct interpretation of the observations.

One of the simplest MHD shear flows is a plane MHD tangential discontinuity. In such a flow, the flow velocity is parallel to the plane, the background quantities are constant on both sides of the plane, while across the plane the quantities possess a jump-type discontinuity. In the case of incompressible plasmas the stability criterion for an MHD tangential discontinuity is rather simple. It was obtained by Syrovatskii (1957)

and Chandrasekhar (1961). The dispersion equation governing the stability of MHD tangential discontinuities in compressible plasmas was obtained by Fejer (1964). The stability criterion in an explicit form can be derived from this dispersion equation only in some particular cases.

When a tangential discontinuity is unstable, the growth rate of the unstable normal modes is proportional to the wave number and, therefore, unbounded. Hence, an initial value problem for an unstable discontinuity is ill-posed. This property is related to the fact that modelling of real flows with strong transverse gradients by introducing discontinuities is unphysical. In reality, at the location of strong gradients there is always a transitional layer of finite thickness in which the background quantities vary strongly but remain continuous. A mathematical treatment of shear flows with transitional layers of finite thickness is considerably more complicated than a treatment of flows with tangential discontinuities. The reason for this is that the linear differential equations one has to deal with have variable coefficients in the former case, while the equations have

constant coefficients in their respective domains in the latter case. As a result, in general, it is impossible to obtain in a closed analytic form a dispersion equation governing the stability of a shear flow possessing a finite transition layer. Instead, the frequency as a function of wavenumber for the eigenmodes for such a flow has to be determined by solving numerically an eigenvalue problem for a differential equation with variable coefficients.

However, there exists one known exception from this general situation. Specifically, when the fluid is incompressible and a shear flow has a piecewise linear profile the linearized stability equations admit a rather simple explicit analytic solution. The existence of such a solution allows one to obtain the dispersion equation explicitly in terms of elementary functions. The main difference between the dispersion equation for flows with the tangential discontinuities and for shear flows of incompressible fluids with the piecewise linear velocity profiles is that the former are polynomial both with respect to the wave frequency ω and the wavenumber k, while the latter are polynomial only with respect to ω and transcendental with respect to k. The stability analysis of simple flows of incompressible fluids with piecewise linear velocity profiles can be found, e.g., in Chandrasekhar (1961) and Drazin & Reid (1981).

In this paper we extend the stability analysis of incompressible flows with piecewise linear velocity profiles to include the effect of magnetic field. Generally, the MHD equations do not admit explicit analytic solutions even when the fluid is incompressible, the magnetic field is uniform and the velocity profile is piecewise linear. There are, however, some particular cases in which such a solution is possible. We treat in the paper one such a case. In this case, it is supposed that a uniform magnetic field is present in the half-space occupied by a motionless plasma, while the half-space occupied by a shear flow is magnetic-free. The velocity profile of the shear flow is piecewise linear. Both the magnetic field and the shear flow are parallel to the dividing plane. For this particular magnetic plasma configuration we obtain a dispersion equation in an explicit form and carry out a stability analysis.

The paper is organized as follows. In the next section we give a formulation of the stability problem and derive the dispersion equation. In Sect. 3, properties of the dispersion equation are addressed. In Sect. 4 a particular case of a magnetic-free flow, with the effect of gravity included, is treated. In Sect. 5 we study the stability of a magnetic flow without gravity and discuss possible applications of the results to the heliopause stability. In Sect. 6, a summary of the results is presented and conclusions are drawn.

2. Problem formulation and derivation of the dispersion equation

We treat stability of the magnetic plasma configuration sketched in Fig. 1. In this configuration, the magnetic field, $\boldsymbol{B}_0(z)$, is in the x-direction of Cartesian coordinates x, y, z, it is uniform and non-zero in the upper half-space, ($z \geq 0$), and
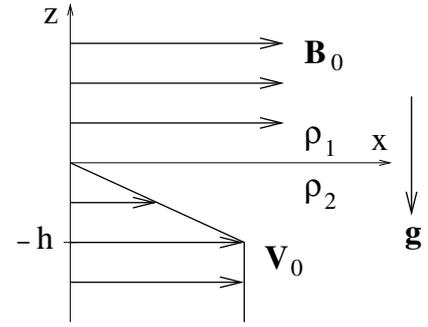
Fig. 1. Sketch of the base state. The gravity acceleration, $\boldsymbol{g}$, is directed downwards when $\rho_1 < \rho_2$, and upwards when $\rho_1 > \rho_2$.

zero in the lower half-space, ($z < 0$). The magnetic field is given by

$$\boldsymbol{B}_0(z) = \widetilde{B}_0(z)\boldsymbol{e}_x, \quad \text{with} \quad \widetilde{B}_0(z) = \begin{cases} B_0, & z \geq 0, \\ 0, & z < 0, \end{cases} \quad (1)$$

where $\boldsymbol{e}_x$ is the unit vector in the positive x-direction and B_0 is a positive constant. The plasma density is equal to

$$\rho(z) = \begin{cases} \rho_1, & z \geq 0, \\ \rho_2, & z < 0, \end{cases} \quad (2)$$

where ρ_1 and ρ_2 are constant and generally $\rho_1 \neq \rho_2$. The plasma velocity is supposed to have the form $\boldsymbol{V}_0 = V_0(z)\boldsymbol{e}_x$, where $V_0(z)$ is given by

$$V_0(z) = \begin{cases} 0, & z \geq 0, \\ -V_m(z/h), & -h \leq z \leq 0, \\ V_m, & z \leq -h, \end{cases} \quad (3)$$

with V_m being a positive constant. The effect of gravity is modelled by assuming that the gravity force represented through the constant gravity acceleration, $\boldsymbol{g}$, is acting in the z-direction: $\boldsymbol{g} = -g\boldsymbol{e}_z$, where $\boldsymbol{e}_z$ is the unit vector in the z-direction and g is a constant.

In the case when $g(\rho_2 - \rho_1) < 0$ the model is always unstable with respect to perturbations propagating in the y-direction owing to the Rayleigh-Taylor instability. As we are interested in the MHD instability related only to the shear velocity profile we exclude the Rayleigh-Taylor instability from the analysis by assuming that $g(\rho_2 - \rho_1) > 0$. Taking into account that the total pressure (which is the sum of the kinetic and magnetic pressures) has to be continuous at $z = 0$, we obtain that the equilibrium pressure, p_0, is given by

$$p_0 = \begin{cases} p_{00} - \rho_1 gz, & z \geq 0, \\ p_{00} - \rho_2 gz + \dfrac{B_0^2}{2\mu}, & z < 0, \end{cases} \quad (4)$$

where p_{00} is an arbitrary constant and μ is the magnetic permeability of vacuum.

In the analysis, we treat only the y-independent perturbations of the base state. Such perturbations are governed by the following system of linearized MHD equations, for $z > 0$ and $z < 0$,

$$\frac{\partial u}{\partial x} + \frac{\partial w}{\partial z} = 0, \quad (5)$$

$$\frac{\partial u}{\partial t} + V_0 \frac{\partial u}{\partial x} + w \frac{dV_0}{dz} = -\frac{1}{\rho}\frac{\partial p}{\partial x}, \tag{6}$$

$$\frac{\partial w}{\partial t} + V_0 \frac{\partial w}{\partial x} = -\frac{1}{\rho}\frac{\partial}{\partial z}\left(p + \frac{\widetilde{B}_0 b_x}{\mu}\right) + \frac{\widetilde{B}_0}{\mu\rho}\frac{\partial b_z}{\partial x}, \tag{7}$$

$$\frac{\partial b_x}{\partial t} = \widetilde{B}_0 \frac{\partial u}{\partial x} - V_0 \frac{\partial b_x}{\partial x} + b_z \frac{dV_0}{dz}, \tag{8}$$

$$\frac{\partial b_z}{\partial t} = \widetilde{B}_0 \frac{\partial w}{\partial x} - V_0 \frac{\partial b_z}{\partial x}. \tag{9}$$

Here u and w are the x and z-components, respectively, of the perturbation velocity, b_x and b_z are the x and z-components, respectively, of the perturbation magnetic field, and p is the perturbation pressure.

The system of Eqs. (5)–(9) has to be supplemented with the boundary conditions at the magnetic interface, ($z = 0$), and at the surface ($z = -h$) where the first derivative of the base velocity profile is discontinuous. Let the equation of the perturbed magnetic interface be $z = \eta(t, x)$. Then the kinematic boundary condition and the continuity condition for the total pressure at $z = 0$ read

$$w_1 = w_2 = \frac{\partial\eta}{\partial t}, \quad \text{and} \tag{10}$$

$$p_1 + \frac{B_0 b_x}{\mu} - \rho_1 g\eta = p_2 - \rho_2 g\eta, \tag{11}$$

respectively. At $z = -h$, the vertical perturbation velocity, w, and the perturbation pressure, p, must be continuous:

$$w_1 = w_2 \quad \text{and} \quad p_1 = p_2. \tag{12}$$

For studying the normal-mode stability of the model, we assume that all the perturbation quantities have the form $\phi(z)\exp(ikx - i\omega t)$, where k is a real-valued wavenumber and ω is a frequency that generally is complex-valued. Substitution of the normal-mode expressions into the system (5)–(9) results in a system of ordinary differential equations in each region, $z < 0$ and $z > 0$, for the amplitudes, $\phi(z)$, of the corresponding perturbation quantities. One eliminates all the dependent variables from the system, except for $w(z)$, and obtains that in both regions, $z < 0$ and $z > 0$, the amplitude of the normal-mode perturbation vertical velocity, $w(z)$, satisfies the equation

$$\frac{d^2 w}{dz^2} - k^2 w = 0. \tag{13}$$

Here and further in the text, the character used for denoting a dependent physical quantity will be used for denoting the normal-mode amplitude of the quantity. In terms of w, the amplitudes of other perturbation variables read

$$u = \frac{i}{k}\frac{dw}{dz}, \quad b_x = -\frac{iB_0}{\omega}\frac{dw}{dz}, \quad b_z = -\frac{kB_0}{\omega}w, \tag{14}$$

$$p = \frac{i\rho}{k}\left(\frac{\omega - kV_0}{k}\frac{dw}{dz} + w\frac{dV_0}{dz}\right). \tag{15}$$

We note that the perturbations have to vanish as $|z| \to \infty$. Under this condition, the general solution of Eq. (13), for $k > 0$, takes the form

$$w = \begin{cases} A_1 e^{-kz}, & z > 0, \\ A_+ e^{kz} + A_- e^{-kz}, & -h < z < 0, \\ A_2 e^{k(z+h)}, & z < -h, \end{cases} \tag{16}$$

where A_1, A_2, A_+ and A_- are arbitrary constants. We treat here only the case $k > 0$. Owing to the symmetry, the results for $k < 0$ are similar. By using (14) and (15) it is straightforward to obtain similar expressions for u, b_x, b_z and p. Substitution of these expressions and of that given by Eq. (16) into the boundary conditions (10) and (11), and in the conditions (12) of continuity of w and p at $z = -h$, results in a system of five linear homogeneous algebraic equations for A_1, A_2, A_+, A_- and η. The condition that this system has a non-trivial solution gives us the dispersion equation of the problem,

$$D_0(\alpha, \Omega) \equiv 2\Omega^3 + 2(\Delta U - \alpha)\Omega^2 + (U - W)\Omega + UW = 0, \tag{17}$$

where $\alpha = kh$ is the dimensionless wave number and the other quantities are

$$s = \frac{\rho_2}{\rho_1}, \quad \Delta = \frac{s-1}{s+1}, \quad \Omega = \frac{\omega h}{V_m(1+\Delta)}, \quad U = \frac{2\alpha - 1 + e^{-2\alpha}}{2(1+\Delta)}, \tag{18}$$

$$W = \frac{\alpha[2R + \alpha H(1-\Delta)]}{(1+\Delta)^2}, \quad R = \frac{gh\Delta}{V_m^2}, \quad H = \frac{B_0^2}{\mu\rho_1 V_m^2}. \tag{19}$$

Here R is the Richardson number and H is the inverse square of the Alfvénic Mach number. Since $g(\rho_2 - \rho_1) > 0$, it holds that $g\Delta > 0$ and hence $R > 0$. We see from (17)–(19) that, for any fixed α and Δ, the only parameter controlling the stability is W. For $\alpha \neq 0$, the latter can vary owing to the variation of R or H. Since $(1 - \Delta) > 0$, under these conditions, for a fixed $\alpha > 0$, the effect of enhancement of the magnetic field, i.e., increase of H, is equivalent to the increase of R for a fixed value of H. The quantity Ω can be considered as a scaled dimensionless frequency. For fixed s, R and H, the frequency, Ω, can be calculated as a function of α by using Eq. (17).

Here it is worth to make one comment. In general, the system of Eqs. (5)–(9) has a singularity in the region $-h < z < 0$ corresponding to a critical layer. The position of this critical layer is determined by the equation $V_0(z) = \omega/k$. In particular, such a singularity was found by Murawski (2000) who studied the effect of flows on the solar f-modes. However, when the velocity profile is linear, the term responsible for the singularity in the Taylor-Goldstein equation (Eq. (15) in Murawski, 2000) disappears, and this equation reduces to Eq. (13). As a result, there is no singularity in the system of Eqs. (5)–(9), and no critical layer in the flow considered in our paper.

3. Properties of the dispersion equation

In this section we address some general properties of the dispersion equation given by Eq. (17). Since the dispersion equation function, $D_0(\alpha, \Omega)$, defined by Eq. (17) is a cubic polynomial with real coefficients with respect to Ω, it has, for any

value of wavenumber, α, and any combination of the parameters involved, either three real Ω-roots, or one real root and two complex conjugate roots. In the former case the flow is stable, and it is unstable in the latter case. The discriminant, D, of $D_0(\alpha, \Omega)$ as a cubic polynomial of Ω is given, up to the factor 4, by

$$
\begin{aligned}
D =\ & 2W^3 + \big[(\alpha - \Delta U)^2 + 18U(\alpha - \Delta U) - 27U^2 \\
& -6U]W^2 + 2U[4(\alpha - \Delta U)^3 - (\alpha - \Delta U)^2 \\
& -9U(\alpha - \Delta U) + 3U]W + U^2[(\alpha - \Delta U)^2 - 2U\big]. \quad (20)
\end{aligned}
$$

Equation (17) has only one real root when $D < 0$ and three real roots when $D \geq 0$ (see e.g. Korn & Korn 1961). Hence, a monochromatic wave with a dimensionless wavenumber α is unstable when $D < 0$ and stable when $D \geq 0$.

    The discriminant, D, is a cubic polynomial with respect to W. When $0 < \alpha \ll 1$, this polynomial has only one real root, W_1^0, given by

$$
W_1^0 = \frac{\alpha^2(1 - \Delta)}{2(1 + \Delta)} + O(\alpha^3). \quad (21)
$$

Therefore, it holds that $D < 0$ when $W < W_1^0$ and $D \geq 0$ when $W \geq W_1^0$. Hence, long waves, i.e., $\alpha \ll 1$, are unstable in the model when $W < W_1^0$ and stable otherwise.

    When $\alpha \gg 1$ the polynomial in (20) has three real roots. One of them is approximately $-1/8$, and the two others are given to the leading order in α by the respective expressions

$$
W_{1,2}^\infty = \frac{(2\alpha - 1)(\alpha - 1 - \Delta/2) \pm 4(1 + \Delta)^{1/2}\alpha^{3/2}e^{-\alpha}}{(1 + \Delta)^2}. \quad (22)
$$

Thus, in this case for $W_2^\infty < W < W_1^\infty$ it holds that $D < 0$ and short waves, i.e., $\alpha \gg 1$, are unstable, whereas for $W < W_2^\infty$ and $W > W_1^\infty$ we have $D \geq 0$ and short waves are stable.

    The number of real roots of the polynomial D given by Eq. (20) is determined by its discriminant $\widetilde{D}$: D has only one real root if and only if $\widetilde{D} < 0$ and three real roots if and only if $\widetilde{D} \geq 0$. From the above results for long- and short-wave approximations it follows that $\widetilde{D} < 0$ when $\alpha \ll 1$, and $\widetilde{D} \geq 0$ when $\alpha \gg 1$. Our numerical computations for a dense representative set of values of $|\Delta| \leq 0.99$ and intermediate values of $\alpha = O(1)$ showed that, in each case considered, there exists a value of α, $\alpha_0(\Delta)$, such that $\widetilde{D} < 0$ for $\alpha < \alpha_0$ and $\widetilde{D} > 0$ for $\alpha > \alpha_0$.

    We also established by using computations that the factor $C = [(\alpha - \Delta U)^2 - 2U]$ in the free term of the cubic polynomial D of W given by Eq. (20), and with it the free term U^2C, is negative and the coefficient of W^2 in D is positive at $\alpha = \alpha_0$. Hence, for the values of α that are slightly greater than α_0, the product of the three real roots of the polynomial D is positive, and their sum is negative implying that there are two negative roots and one positive. By using the expression for U given in (18) one obtains that $C \approx -\alpha^2/2$ for $0 < \alpha \ll 1$, $C \approx \alpha^2/(1 + \Delta)^2$ for $\alpha \gg 1$, and the function $dC/d\alpha$ has only one positive zero. This implies that C as a function of α also has only one positive zero which we denote by α_c. We have $C < 0$ for $0 < \alpha < \alpha_c$ and $C > 0$ for $\alpha > \alpha_c$. Since $C(\alpha_0) < 0$, it follows that $\alpha_0 < \alpha_c$. We know that, for $\alpha \gg 1$, there are two positive roots and one
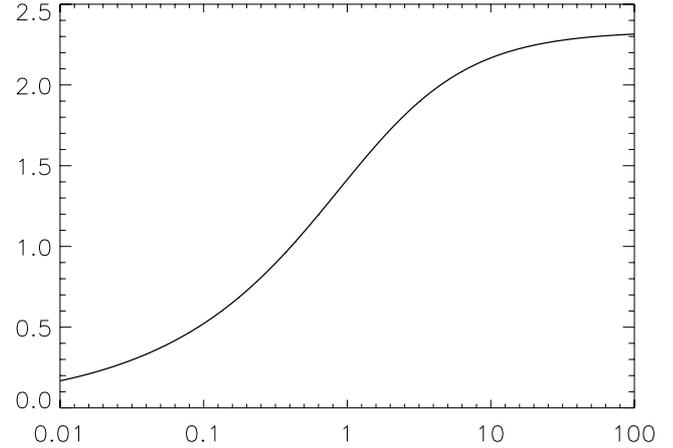

Fig. 2. α_c as a function of s. The s-axis is logarithmic.

negative (see (22)). Since the roots are continuous functions of α, it follows that the number of positive and negative roots can change when α varies only if one of the roots becomes zero at a pariticlar value of α. Since $C > 0$ for $\alpha > \alpha_c$, we know that this does not happen when α decreases from $\alpha \gg 1$ to α_c. Hence, we conclude that there are two positive and one negative root for $\alpha > \alpha_c$.

    From the above consideration of $\widetilde{D}$ and C, and of the dependence of the real roots of D on the signs of $\widetilde{D}$ and C, we obtain that the polynomial D has only one real positive root when $0 < \alpha < \alpha_0$, two negative roots and one positive root when $\alpha_0 < \alpha < \alpha_c$, and one negative root and two positive roots when $\alpha > \alpha_c$.

    Since $W > 0$, we are only interested in positive roots of the polynomial D. Summarizing our analysis we conclude that D has one positive root, W_1, when $\alpha < \alpha_c$, and two positive roots, W_1 and W_2 (with $W_2 < W_1$.) when $\alpha > \alpha_c$. The dependence of α_c on s is shown in Fig. 2. The implication of this results for the flow stability formulated in terms of the parameter W is as follows. Each normal mode with $\alpha < \alpha_c$ is unstable when $W < W_1$ and stable when $W > W_1$; each normal modes with $\alpha > \alpha_c$ is unstable when $W_2 < W < W_1$ and stable when either $W < W_2$ or $W > W_1$.

4. Stability of a magnetic-free flow

In this section we study the flow stability in the absence of magnetic field, i.e., $H = 0$. Stability of similar flows was studied by Chandrasekhar (1961) and Drazin & Reid (1981).

    We start the analysis by treating the case $R = 0$, i.e., $W = 0$. In this case, the dispersion equation, $D_0(\alpha, \Omega) = 0$, has for each α the roots

$$
\begin{aligned}
\Omega_1 &= 0, \quad \text{and} \quad \Omega_{2,3} = \frac{\alpha - \Delta U}{2} \pm \frac{1}{2}\sqrt{C} \\
&= \frac{\alpha - \Delta U}{2} \pm \frac{1}{2}\sqrt{(\alpha - \Delta U)^2 - 2U}.
\end{aligned} \quad (23)
$$

We established in the previous section that $C < 0$ for $0 < \alpha < \alpha_c$ and $C > 0$ for $\alpha > \alpha_c$. Therefore, the normal modes with $0 < \alpha < \alpha_c$ are unstable and with $\alpha > \alpha_c$ are stable. The growth rate of the unstable normal modes, $\gamma = \Im(\Omega)$,
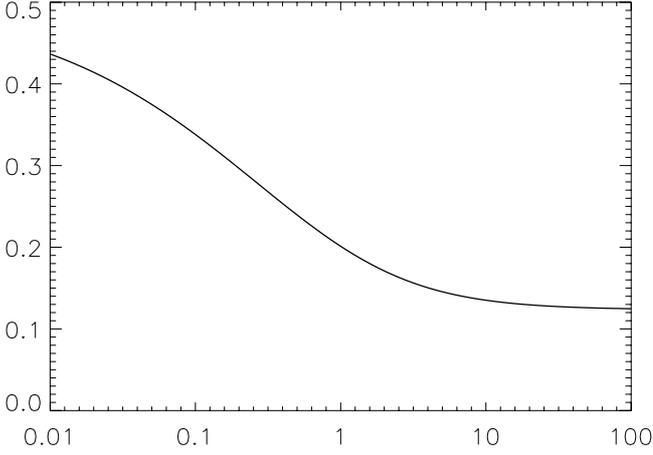
Fig. 3. The maximum growth rate, γ_M, as a function of s for the case $R = 0$. The s-axis is logarithmic.

where $\Im$ indicates the imaginary part of a quantity, is given by

$$\gamma = \frac{1}{2}\left[2U - (\alpha - \Delta U)^2\right]^{1/2}. \tag{24}$$

The function $\gamma = \gamma(\alpha)$ satisfies $\gamma(\alpha_c) = 0$, and by using the expression for U given in (18) one can show that $\gamma(\alpha)$ has exactly one maximum, γ_M, in the interval $[0, \alpha_c]$. The dependence of γ_M on s is shown in Fig. 3. We note that $\Delta = 0$ when $s = 1$ and, in such a case, from (19) it follows that $R = 0$ for any value of g.

We now proceed to treating the case $R \neq 0$. Since $H = 0$, it holds that $W = 2\alpha R(1+\Delta)^{-2}$, see (19). Let $R_{1,2} = \frac{1}{2}\alpha^{-1}W_{1,2}(1+\Delta)^2$, where $W_{1,2}$ are defined at the end of Sect. 3. Then from the results of that section it follows that (i) the normal modes with $\alpha < \alpha_c$ are unstable when $R < R_1$ and stable when $R > R_1$, and (ii) the normal modes with $\alpha > \alpha_c$ are unstable when $R_2 < R < R_1$ and stable when either $R < R_2$ or $R > R_1$.

When $\alpha \ll 1$, R_1 is given by

$$R_1 = \frac{\alpha}{4}\left(1 - \Delta^2\right) + O\left(\alpha^2\right). \tag{25}$$

When $\alpha \gg 1$, R_1 and R_2 are given by the approximate expressions

$$R_{1,2} = \frac{(2\alpha - 1)(2\alpha - 2 - \Delta)}{4\alpha} \pm 2(1 + \Delta)^{1/2}\alpha^{1/2}e^{-\alpha}, \tag{26}$$

respectively. It follows from Eqs. (25) and (26) that R_1 is a monotonically increasing function of α for $\alpha \ll 1$ and $\alpha \gg 1$, and R_2 is a monotonically increasing function of α for $\alpha \gg 1$. Our computations showed that R_1 and R_2 are monotonically increasing functions of α for all intermediate values of α. The neutral curves $R = R_1(\alpha)$ and $R = R_2(\alpha)$ are presented in Fig. 4 for different values of s.

Since the functions $R = R_1(\alpha)$ and $R = R_2(\alpha)$ are monotonically increasing, there exist the respective inverse functions, $\alpha = \alpha_1^R(R)$ and $\alpha = \alpha_2^R(R)$, and these latter are also monotonically increasing functions of their argument. When R is fixed, a normal mode with the wavenumber α is unstable if $\alpha_1^R(R) < \alpha < \alpha_2^R(R)$, while it is stable if either $\alpha < \alpha_1^R(R)$ or

$\alpha > \alpha_2^R(R)$. The dependence of the dimensionless growth rate γ on α is shown in Fig. 5 for $R = 1$ and four different values of s. This dependence is qualitatively the same for all the values of R and s treated.

We also calculated the dependence of the maximum growth rate of the unstable normal modes, $\gamma_M = \max_\alpha[\gamma(\alpha)]$, on R. This dependence is shown in Fig. 6 for different values of s. The curves for large and small values of s have different qualitative features. For large values of s, $\gamma_M(R)$ is a monotonically decreasing function of R, while for small s it possesses a maximum. It can be shown by using Eq. (26) that $\gamma_M \approx \frac{1}{2}R^{1/2}(1 + \Delta)^{1/2}e^{-R}$ when $R \gg 1$.

5. Stability of a magnetic flow without gravity

In this section we study the flow stability in the presence of magnetic field ($H \neq 0$), but without gravity ($R = 0$).

In this case $W = \alpha^2 H(1-\Delta)/(1+\Delta)^2$. We introduce the notation $H_{1,2} = \alpha^{-2}W_{1,2}(1+\Delta)^2/(1-\Delta)$, where $W_{1,2}$ are the positive W−roots of the polynomial D defined in Sect. 3. Then from the results of that section it follows that (i) a normal mode with $\alpha < \alpha_c$ is unstable when $H < H_1$ and stable when $H > H_1$, and (ii) a normal mode with $\alpha > \alpha_c$ is unstable when $H_2 < H < H_1$ and stable when either $H < H_2$ or $H > H_1$. When $\alpha \to 0$ it holds that $H_1 \to \frac{1}{2}(1 + \Delta) = s/(1 + s)$. The criterion for instability in this limit, i.e., $H < H_1$, can be rewritten in the dimensional variables as $V_m^2 > V_{KH}^2 = B_0^2(\rho_1+\rho_2)/(\mu\rho_1\rho_2)$, where V_{KH} is the Kelvin-Helmholtz threshold velocity, see Eqs. (18), (19). This result is in compliance with the classical result on the Kelvin-Helmholtz instability: the limit $\alpha \to 0$, for a fixed non-zero k, corresponds to a tangential discontinuity ($h = 0$), which is stable when $V_m < V_{KH}$ and unstable otherwise (see e.g., Syrovatskii 1957; Chandrasekhar 1961).

When $\alpha \gg 1$, H_1 and H_2 are given by the corresponding approximate expressions

$$H_{1,2} = \frac{1}{1 - \Delta}\left[\left(2 - \frac{1}{\alpha}\right)\left(1 - \frac{2 + \Delta}{2\alpha}\right) \pm 4e^{-\alpha}\left(\frac{1 + \Delta}{\alpha}\right)^{1/2}\right], \tag{27}$$

with $H_1 > H_2$. Computations showed that, for $|\Delta| \leq 0.99$, the quantities H_1 and H_2 are monotonically growing functions of α. The dependence of H_1 and H_2 on α is shown in Fig. 7 for different values of s.

It follows from equation (27) that $H_{1,2} \to 2/(1 - \Delta) = 1 + s$ as $\alpha \to \infty$. Since both H_1 and H_2 are monotonically growing functions of α, it holds that $H_{1,2} < 1 + s$ for any value of α. This implies that all the normal modes in the flow are stable when $H > 1 + s$, while for any $H < 1 + s$ there exist unstable normal modes in the flow. In the dimensional variables the stability criterion, i.e., $H > 1 + s$, is written as

$$V_m^2 < \frac{B_0^2}{\mu(\rho_1 + \rho_2)} = \frac{s}{(1 + s)^2}V_{KH}^2 \stackrel{\text{def}}{=} V_c^2, \tag{28}$$

see Eqs. (18), (19). From Eq. (28) it follows that the presence of a transitional layer with a continuous variation of the velocity strongly reduces the instability threshold, V_c. The ratio of the instability threshold for the continuous flow, V_c, to the instability threshold for the tangential discontinuity, V_{KH}, is equal to
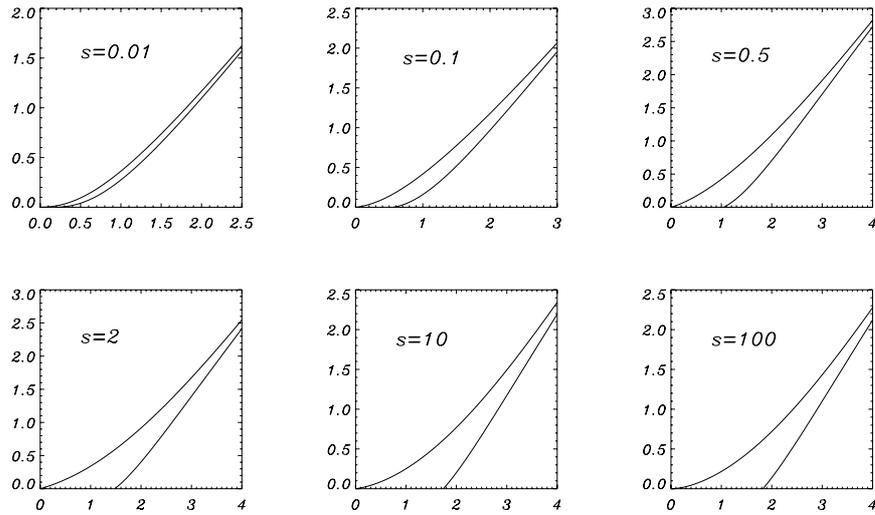
Fig. 4. Graphs of $R = R_1(\alpha)$ (*upper curves*) and $R = R_2(\alpha)$ (*lower curves*) for several values of s. A normal mode with the wavenumber α is unstable if the point (α, R) is in the region between the curves and stable otherwise.
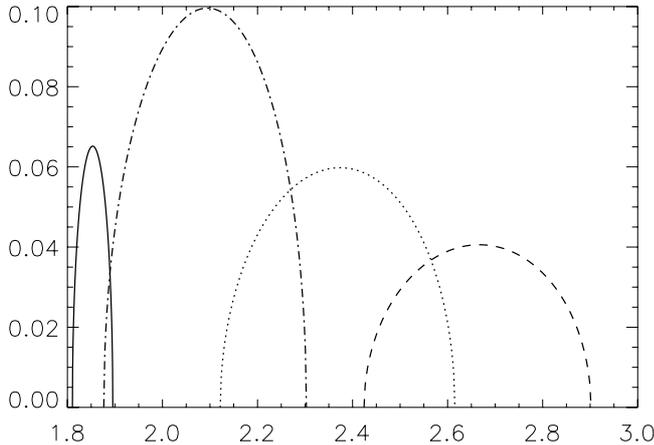
Fig. 5. Growth rate γ as a function of α for $R = 1$ and four different values of s. The dashed, dotted and dash-dotted curves correspond to $s = 100$, $s = 2$ and $s = 0.5$ respectively, the solid curve shows $0.1 \times \gamma$ for $s = 0.01$.

$\sqrt{s}/(1 + s)$. Hence, V_c/V_{KH} is equal to 1/2 for $s = 1$, to 0.2875 for $s = 0.1$ and $s = 10$, and to 0.099 for $s = 0.01$ and $s = 100$.

Since the functions $H_1(\alpha)$ and $H_2(\alpha)$ are monotonically increasing, the inverse functions $\alpha_1^H(H)$ and $\alpha_2^H(H)$ to $H_1(\alpha)$ and $H_2(\alpha)$, respectively, are monotonically increasing as well. When $H < s/(s + 1)$, the normal modes with α satisfying $0 < \alpha < \alpha_2^H(H)$ are unstable, while the normal modes with α satisfying $\alpha > \alpha_2^H(H)$ are stable. When $s/(s+1) < H < 1+s$, the normal modes with α satisfying $\alpha_1^H(H) < \alpha < \alpha_2^H(H)$ are unstable, while the normal modes with α satisfying either $\alpha < \alpha_1^H(H)$ or $\alpha > \alpha_2^H(H)$ are stable.

The dependence of the growth rate, γ, on α is qualitatively somewhat similar to that shown in Fig. 5, though there are two differences. The first difference is that, in the present case, the left boundary of the instability interval is at $\alpha = 0$ when $H < s/(s+1)$. The second one is that, for the values of H that are not much greater than $s/(s+1)$, the curves do not look as symmetric

as those in Fig. 5, whereas their maxima are shifted to the right boundary of the instability domain. Since these differences are quite minor, we do not present the plots of γ versus α.

In Fig. 8 the dependence of the maximum growth rate with respect to α, $\gamma_M = \max_a[\gamma(\alpha)]$, on H is shown for several values of s. Similar to the case shown in Fig. 6, in the present case $\gamma_M(H)$ is a monotonically decreasing function of H for large values of s, while for small s it possesses a maximum. For the values of H that are slightly below the instability threshold, i.e., $H = 1 + s - \delta$, where $0 < \delta \ll 1$, we have

$$\gamma_M \approx \left[\frac{(s + 1)(2s + 1)}{8s\delta} \right]^{1/2} \exp\left(-\frac{2s + 1}{\delta} \right). \qquad (29)$$

Interestingly enough, from the left panel of Fig. 8 it is seen that for $s = 0.01$ and $s = 0.05$ weaker magnetic field, i.e., $H \to 0$, renders the model generally less unstable because in this limit γ_M decreases.

As an example of application of the obtained results we consider the stability of the heliopause. When the supersonic flow of the solar wind interacts with the supersonic flow of the interstellar medium an interaction region is formed. This region is bounded by the bow shock that decelerates and compresses the interstellar medium flow and by the termination shock that decelerates and compresses the solar wind flow (see e.g. Baranov et al. 1970, 1976; Baranov 1990). Between these two shocks there is a region with a strong transverse gradient of the velocity component parallel to the shocks. This region, called the heliopause, can be, and is often, modeled as a sort of a tangential discontinuity separating the decelerated interstellar medium and the solar wind. A similar region is formed when two stellar winds collide in a binary star system (see e.g. Myasnikov & Zhekov 1991, 1993, 1998).

To our knowledge, the heliopause stability was first treated by Fahr et al. (1986). Following that work, the problem of the heliopause stability received a considerable attention in the literature. A recent review of the studies on the heliopause stability can be found in Ruderman (2000).
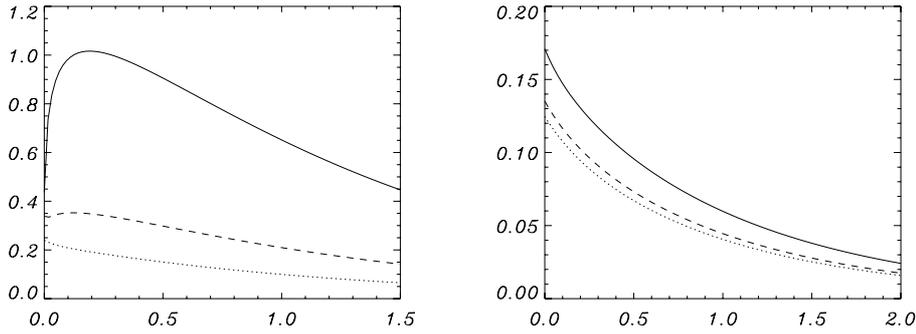
Fig. 6. Maximum growth rate, $\gamma_M = \max_\alpha[\gamma(\alpha)]$, as a function of R for six values of s. The solid, dashed and dotted curves correspond to $s = 0.01$, $s = 0.1$ and $s = 0.5$, respectively, in the left panel, and to $s = 2$, $s = 10$ and $s = 100$, respectively, in the right panel.
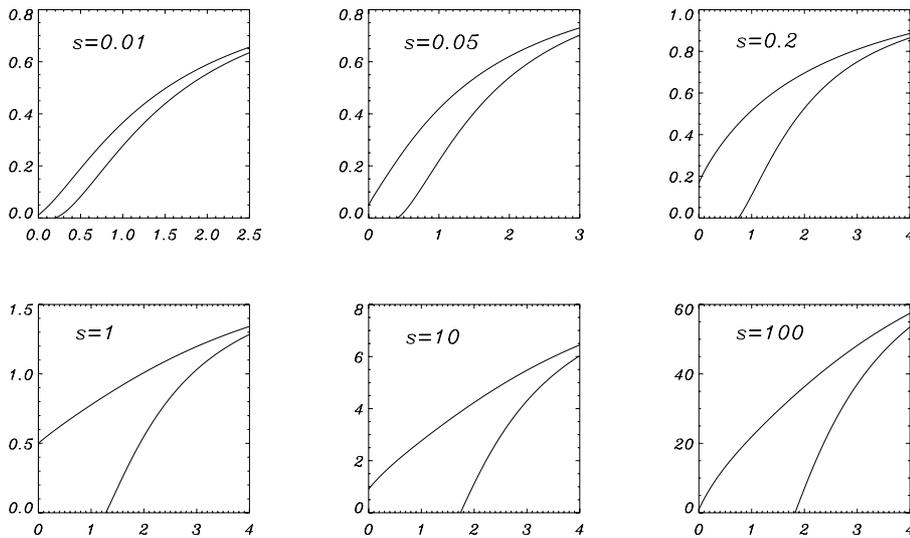
Fig. 7. Graphs of $H = H_1(\alpha)$ (upper curves) and $H = H_2(\alpha)$ (lower curves) for several values of s. A normal mode with the wavenumber α is unstable if the point (α, H) is in the region between the curves and stable otherwise.
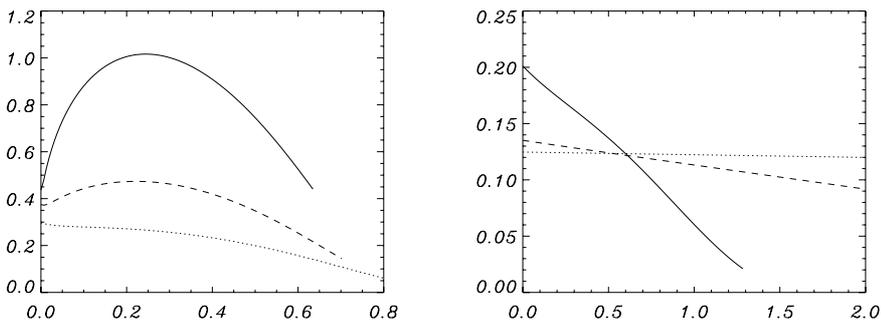
Fig. 8. Maximum growth rate, $\gamma_M = \max_\alpha[\gamma(\alpha)]$, as a function of H for six values of s. The solid, dashed and dotted curves correspond to $s = 0.01$, $s = 0.05$ and $s = 0.2$ respectively in the left panel, and to $s = 1$, $s = 10$ and $s = 100$ respectively in the right panel.

In their study, Fahr et al. (1986) discussed, in particular, the effect of the interstellar magnetic field on the heliopause stability. They considered a portion of the interaction region close to the apex point. In this portion, the flows of the decelerated interstellar medium and the solar wind are strongly subsonic, and hence the fluid can be treated as being incompressible. The heliopause was modeled by Fahr et al. (1986) as a true discontinuity and, thus, they applied the stability criterion for an MHD tangential discontinuity in an incompressible ideal fluid. If one

neglects the magnetic field of the solar wind then, according to this criterion, the discontinuity is stable if and only if the velocity jump at the discontinuity, V_m, satisfies the inequality $V_m < V_{KN} = B_0 \sqrt{(\rho_1 + \rho_2)/(\mu\rho_1\rho_2)}$.

A typical value of the density ratio of the solar wind and the interstellar medium compressed at the shocks is $s = 0.01$. The velocity variation, V_m, through the heliopause ranges from zero to about 75 km s^{-1} in the portion of the interaction region where the flow can be considered as incompressible (see

e.g. Baranov et al. 1976; Ruderman et al. 2004). A typical value of the electron number density in the interstellar medium is about 0.1 cm^{-3}. Since the bow shock is supposed to be weak, this value can also be taken as being typical for the electron density in the interstellar medium behind the shock. From here the density of the interstellar plasma is estimated as $\rho_1 \approx 1.7 \times 10^{-25}$ g cm^{-3}. Given this, we obtain by using the stability criterion for a true discontinuity, $V_m < V_{KH}$, that the portion of the interaction region where the flow can be considered as incompressible is stable if and only if the magnitude of the interstellar magnetic field, B_0, is greater than about 10^{-6} G. There are indications that the fields of such a magnitude or even of greater magnitudes exit in the interstellar medium (see e.g. Frisch 1989).

However, if we relax the assumption that the heliopause is a true tangential discontinuity and instead use the continuous model of the present paper then the stabilization result is quite different. In the continuous case, the heliopause is stable if and only if $V_m < V_c = B_0/\sqrt{\mu(\rho_1 + \rho_2)}$, see (28). Therefore, for the heliopause to be stable, B_0 has to be greater than about 10^{-5} G. The magnetic field of a lower order of magnitude can destabilize the heliopause. This can be seen, for instance, from Fig. 8 showing the maximum growth rate of the normal modes, γ_M, as a function of H. For $s = 0.01$, the function $\gamma_M(H)$ attains its maximum at $H \approx 0.205$. From (19) it follows that for this value of H the value of B_0 varies from zero to about 5×10^{-6} G when V_m is varying from zero to 75 km s^{-1}. Consequently, the stability threshold for the magnetic field of the heliopause predicted based on a true discontinuity assumption, i.e., $B_0 \approx 10^{-6}$ G, is by one order of magnitude lower than that obtained within the present continuous layer model, i.e., $B_0 \approx 10^{-5}$ G.

6. Summary and conclusions

In this paper, we studied the linear stability of a simple shear flow of an incompressible fluid with a continuous piecewise linear velocity profile in the presence of gravity and magnetic field. An explicit expression for the dispersion equation governing the linear flow stability was derived and its main properties were investigated. We treated separately the case where there is gravity but no magnetic field, and then the case where there is a magnetic field but no gravity. An analytical and a numerical approaches were combined to obtain the neutral curves in the wavenumber–Richardson number plane in the first case, and in the wavenumber–inverse squared Alfvénic Mach number plane in the second case. We also analysed the dependence of the growth rate of the unstable normal modes on the Richardson number in the first case, and on the inverse squared Alfvénic Mach number in the second case.

The most interesting result obtained in our analysis is that introducing a transitional layer with the varying velocity magnitude in place of a true tangential discontinuity destabilizes the flow. The flow without a transitional layer (MHD tangential discontinuity) is unstable if and only if the velocity jump, V_m, is greater than the Kelvin-Helmholtz threshold velocity, V_{KH}, whereas the flow with a transitional layer is unstable if and only if V_m is greater than a lower threshold, specifically $V_m > V_c$, where $V_c = \sqrt{s}V_{KH}/(1 + s) < V_{KH}$, with s being the density ratio of the magnetic-free and magnetic domains of the flow.

We applied the results to the stability of a strongly subsonic portion of the heliopause. Our main conclusion is that the previously obtained estimates for the interstellar magnetic field, B_0, required to stabilize this portion of the heliopause have to be revised. The presence of a transitional layer increases the estimate for the value of B_0 by one order of magnitude in comparison to that obtained on the basis of modelling the heliopause as a tangential discontinuity.

References

Baranov, V. B. 1990, Space Sci. Rev., 52, 89
Baranov, V. B., Krasnobaev, K. V., & Kulikovski, A. G. 1970, Sov. Phys. Dokl. (in Russian), 15, 791
Baranov, V. B., Krasnobaev, K. V., & Ruderman, M. S. 1976, Ap&SS, 41, 481
Chandrasekhar, S. 1961, Hydrodynamic and Hydromagnetic Stability (Oxford: Clarendon Press)
Drazin, P. G., & Reid, W. H. 1981, Hydrodynamic Stability (Cambridge: Cambridge Univ. Press)
Fahr, H. J., Neutsch, W., Grzedzielski, S., Macek, W., & Ratkiewicz, R. 1986, Space Sci. Rev., 43, 329
Fejer, J. 1964, Phys. Fluids, 7, 499
Frisch, P. C. 1989, Physics of the Outer Heliosphere, COSPAR Colloquia Series, 1, 19
Korn, G. A., & Korn, T. M. 1961, Mathematical Handbook for Scientists and Engineers (New York: McGraw-Hill)
Murawski, K. 2000, ApJ, 537, 495
Myasnikov, A. V., & Zhekov, S. A. 1991, Ap&SS, 184, 287
Myasnikov, A. V., & Zhekov, S. A. 1993, MNRAS, 260, 221
Myasnikov, A. V., & Zhekov, S. A. 1998, MNRAS, 300, 686
Ruderman, M. S. 2000, Ap&SS, 274, 327
Ruderman, M. S., Brevdo, L., & Erdélyi, R. 2004, Proc. R. Soc. Lond. A, 460, 847
Syrovatskii, S. I. 1957, Usp. Fiz. Nauk (in Russian), 62, 247